*Proceedings of the*
*Annual Stability Conference*
*Structural Stability Research Council*
*Grapevine, Texas, April 18-21, 2012*

# On the Behavior, Failure and DSM Design of Thin-Walled Steel Frames

C. Basaglia[1] and D. Camotim[1]

## Abstract

This paper reports the available results of an ongoing numerical investigation on the buckling, post-buckling, collapse and design of simple frames. The results presented and discussed are obtained through analyses based on Generalized Beam Theory (elastic buckling analyses) and shell finite element models (elastic and elastic-plastic post-buckling analyses). Moreover, the ultimate loads obtained are used to establish preliminary guidelines concerning the design of steel frames failing in modes that combine local, distortional and global features. An approach based on the existing Direct Strength Method (DSM) strength equations is followed and the comparison between the numerical and predicted ultimate loads makes it possible to draw some interesting conclusions concerning the issues that must be addressed by a DSM design procedure that can be successfully applied to thin-walled steel frames.

## 1. Introduction

The extensive use of thin-walled steel frames in the construction industry stems mostly from their high structural efficiency (large strength-to-weight ratio), remarkable fabrication versatility and very low production and erection costs. However, since these steel framed structures are usually built from open-section members (*e.g.*, cold-formed columns and beams), which are highly prone to local, distortional and global buckling phenomena, the direct assessment of their structural response constitutes a rather complex task (*e.g.*, Dubina 2008). Therefore, such steel frames are currently designed by means of an indirect approach, basically consisting of (i) "extracting" the various members from the frame (more or less adequately) and then (ii) safety checking them individually as "isolated members". The main shortcoming (source of error/approximation) of this approach stems from the inadequate accounting of the "real behavior" of the frame joints – indeed, the "extracted" members are almost always safety checked under the assumption of standard support conditions (pinned or fixed end sections) and the only "link" to the original frame is the member "effective/buckling length", a concept initially devised in the context of the in-plane flexural buckling of isolated members and later extended to handle the geometrically non-linear in-plane frame behavior. In particular, no attention is paid to several important frame joint behavioral features, such as those associated with the (i) warping torsion transmission (*e.g.*, Basaglia *et al.* 2012), (ii) localized displacement restraints due to bracing systems or connecting devices (*e.g.*, Camotim *et al* 2008) or (iii) local/global displacement compatibility (*e.g.*, Camotim *et al.* 2010). In order to overcome the above shortcoming, Part 1-1 of Eurocode 3 (EC3-1-1 – CEN 2005) proposes (allows for) the use of a

[1] ICIST, Instituto Superior Técnico, Technical University of Lisbon, Portugal.
<cilmarbasaglia@gmail.com>, <dcamotim@civil.ist.utl.pt>

so-called "General Method", which is intended for the design a wide variety of structural systems, even if no proper validation results or application guidelines are provided – this explains why several European Community countries either completely forbid or severely restricted its application in their EC3 National Annexes. Quite recently, Bijlaard *et al.* (2010) investigated the application of this method to the design of plane frames against spatial global failure (*i.e.*, collapse mechanisms involving lateral-torsional buckling).

In the last few years, a fair amount of research work has been devoted to the development of efficient design rules for isolated (single-span) thin-walled steel members, mostly subjected to uniform internal force and moment diagrams. The most successful end product of this intense research activity is the Direct Strength Method (DSM), which (i) has its roots in the work of Hancock *et al.* (1994), (ii) was originally proposed by Schafer and Peköz (1998) and (iii) has been continuously improved since then (*e.g.*, Schafer 2008). Following the universal acceptance of the DSM approach to design cold-formed steel members, it has already been included in the latest versions of the corresponding North American (AISI 2007) and Australian/New Zealand (AS/NZS 2005) specifications.

The aim of this work is to present and discuss the results of an ongoing numerical investigation on the local, distortional and global buckling, post-buckling, collapse and DSM design of simple frames. The numerical results presented were obtained through (i) Generalized Beam Theory (GBT) buckling analyses and (ii) elastic and elastic-plastic shell finite element (SFE) post-buckling analyses. In particular, some interesting conclusions are drawn on the features that must be incorporated in a DSM design procedure for this type of thin-walled steel structural systems.

## 2. Numerical Investigation: Scope and Modeling Issues

Fig. 1 shows the dimensions of the plain channel, lipped channel and I-section exhibited by the frame members dealt with in this work – all have elastic constants $E=205\ GPa$ (Young's modulus) and $\upsilon=0.3$ (Poisson's ratio). Figs. 2 to 4 depict the main features of the deformation modes that are more relevant for the GBT buckling analyses carried out throughout the paper (*i.e.*, those with significant contributions to the frame buckling mode shapes).

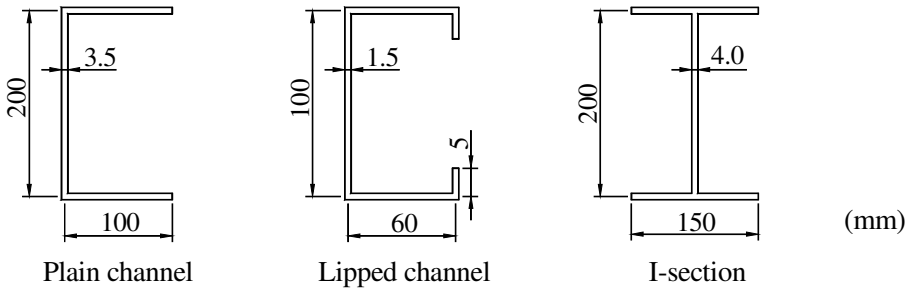


Figure 1: Plain channel, lipped channel and I-section dimensions.

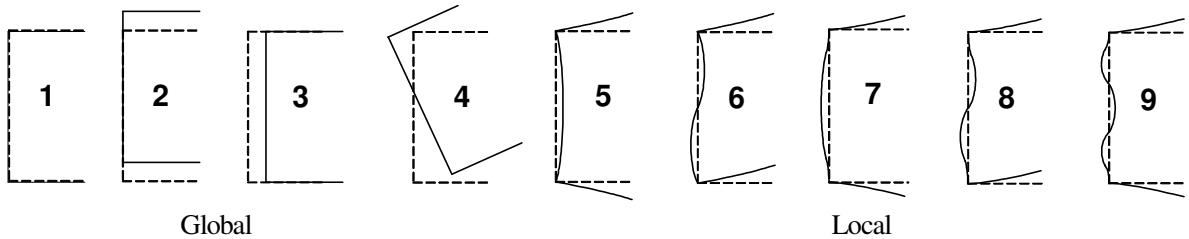


Figure 2: Main features of the most relevant plain channel deformation modes.

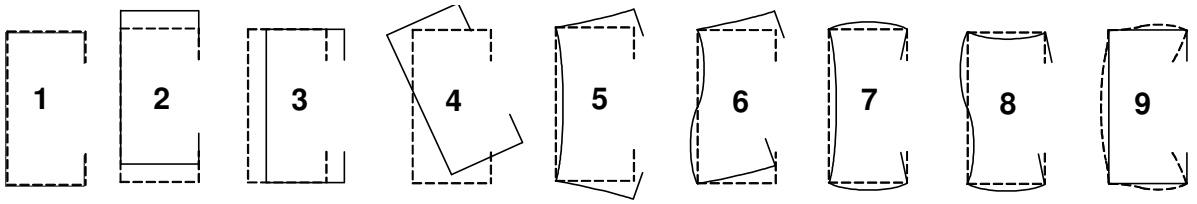


Figure 3: Main features of the most relevant lipped channel deformation modes.

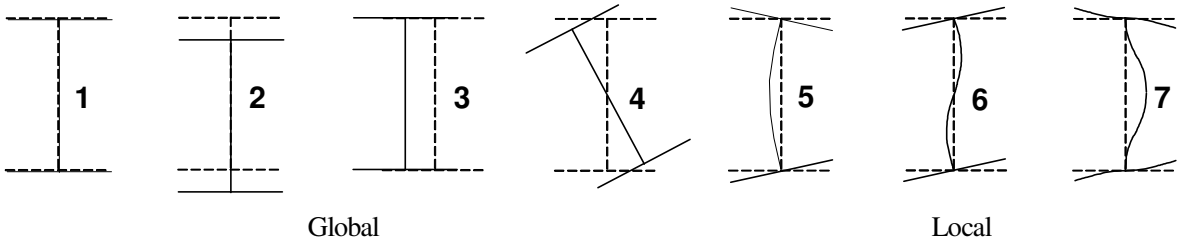


Figure 4: Main features of the most relevant I-section deformation modes.

The buckling, post-buckling and ultimate strength results presented next concern the non-linear behaviors of the frames shown in Figs. 5 to 7. The "L-shaped" plane frame depicted in Fig. 5 (termed LF-U) is formed by two orthogonal short members exhibiting (i) identical plain channel cross-sections (see Fig. 1), (ii) fixed end sections with warping prevented, and (iii) flange continuity at the joint (*i.e.*, the two members are connected with their flanges lying in the same plane) – the members (A and B) have the same length ($L_A$=$L_B$=*70cm*) and are unequally axially compressed ($N_A$=$Q$ and $N_B$=*0.8*$Q$, where $Q$ is the load parameter) – naturally, this setting "forces" the collapse to occur in member A. The symmetric orthogonal portal frame displayed in Fig. 6 (termed PF-C) (i) is formed by three members with identical lipped channel cross-sections (see Fig. 1), (ii) has fixed column bases and joints with flange continuity, and (iii) is acted by four loads applied at the joints and causing only first-order member axial forces ($N_A$=$N_C$=*0.83*$Q$ and $N_B$=$Q$). Finally, Fig. 7 shows a second "L-shaped" plane frame (termed LF-I), now formed by two fairly long members ($L_A$=*400cm* and $L_B$=*600cm*) exhibiting (i) identical I cross-sections (see Fig. 1), (ii) again fixed end sections with warping prevented, and (iii) a box-stiffened joint (web continuity) – the frame is subjected to a vertical load $Q$ applied at the beam mid-span cross-section centroid, causing essentially (i) bending in member B (beam) and (ii) bending and axial compression in member A (beam-column). Note that the geometries of these three frames were chosen in order to ensure buckling and failure modes involving all types of deformations (local, distortional and global).

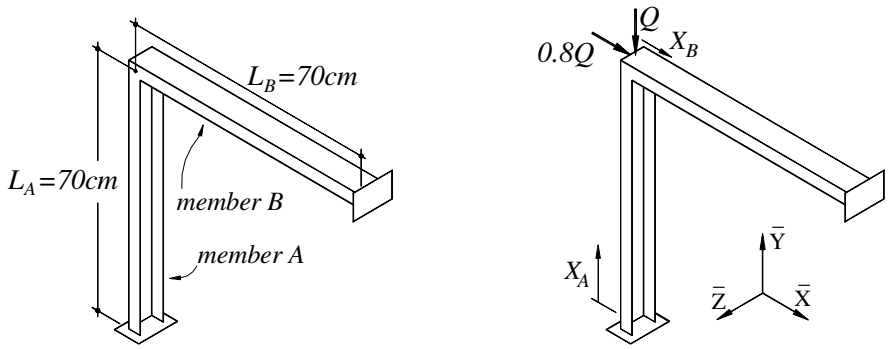


Figure 5: "L-shaped" frame formed by plain channel members (LF-U): geometry, loading and support conditions.

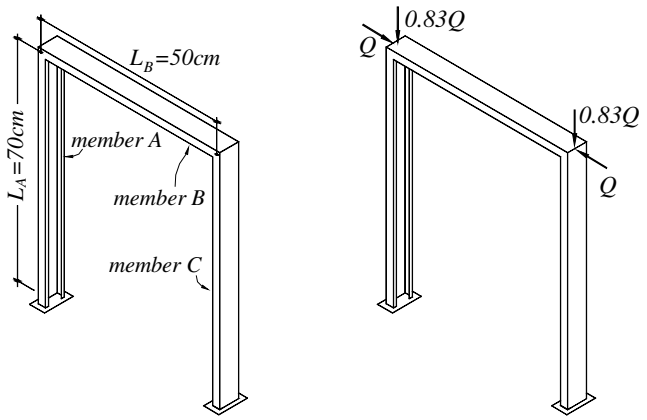


Figure 6: Symmetric portal frame (PF-C): geometry, loading and support conditions.

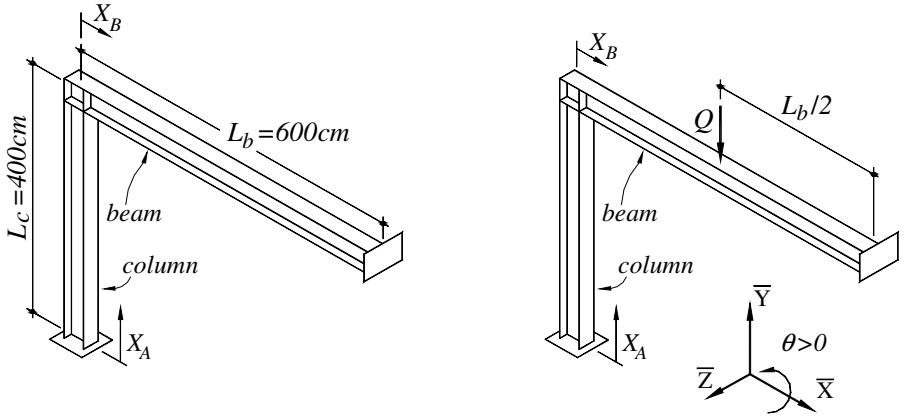


Figure 7: "L-shaped" frame formed by I-section members (LF-I): geometry, loading and support conditions.

Concerning the GBT and SFE analyses, the following modeling issues deserve to be mentioned:

(i) *GBT Discretization*. The GBT buckling equilibrium equations were solved using the beam finite element originally developed by Bebiano *et al.* (2007) and subsequently enhanced by Basaglia *et al.* (2010) – it is worth noting that the formulation of this element takes into account the geometrical effects stemming from the longitudinal normal stress gradients and ensuing pre-buckling shear stresses, thus enabling the appropriate capture of shear buckling effects.

(ii) *SFE Discretization*. The elastic and elastic-plastic SFE post-buckling analyses were performed in the commercial code ANSYS (SAS 2009) and based on frame discretizations into fine meshes of 4-node Shell181 finite elements.

(iii) *Material Modeling*. The steel material behavior is deemed either linear elastic (bucking analyses) or linear-elastic/perfectly-plastic with the von Mises yield criterion and its associated flow rule (post-buckling analyses). This means that ($iii_1$) no strain hardening is taken into account and ($iii_2$) it is assumed that there exists enough ductility to allow for all the stress redistributions that occurs prior to the frame collapse.

(iv) *Initial Imperfections*. Critical-mode initial geometrical imperfections with amplitude equal to either *10%* of the wall thickness (local or distortional buckling) or *L/1000* (global buckling), values that are often adopted in numerical simulations carried out by thin-walled steel researchers – a more judicious choice requires the performance of imperfection-sensitivity studies, which falls outside the scope of this paper. Moreover, no residual stresses are included in the analyses.

## 3. Buckling Results

In all existing design procedures, a crucial step consists of identifying the buckling mode nature, a task by no means straightforward in thin-walled frames. This can be confirmed by examining Figs. 8 to 10, which provide two representations of critical buckling mode shapes of the three frames considered in this work, namely (i) ANSYS 3D views and (ii) GBT modal amplitude functions. The corresponding frame critical buckling loads, yielded by GBT and ANSYS analyses, are the following: (i) $Q_{cr.GBT}$=*254.83kN* and $Q_{cr.ANSYS}$=*250.41kN*, for the LF-U frame, (ii) $Q_{cr.GBT}$=*51.66kN* and $Q_{cr.ANSYS}$=*51.37kN*, for the PF-C frame, and (iii) $Q_{cr.GBT}$=*51.32kN* and $Q_{cr.ANSYS}$=*51.83kN*, for the LF-I frame. The analysis of these frame buckling results prompts the following remarks:

(i) The GBT and ANSYS critical buckling loads practically coincide – the maximum difference is *1.7%* and concerns the LF-U frame. There is also very close agreement between the critical buckling mode representations provided by the two analyses.

(ii) While the LF-U frame buckles in a pure local mode, the SF-C and LF-I frame critical buckling modes are "mixed", in the sense that they combine two types of deformation modes: ($ii_1$) local and distortional (PF-C), or ($ii_2$) local and global (LF-I).

(iii) The LF-U and PF-C frames can be more accurately described as sets of rigidly connected columns, since, in practical terms, all their members are axially compressed. Thus, they exhibit a "column-like" buckling behavior that is triggered by the column with the "worst" combination of axial load and end support conditions: ($iii_1$) member A in the LF-U case and ($iii_2$) member B in the PF-C case.

(iv) On the other hand, the buckling behavior of the LF-I frame, which exhibits a "real frame behavior" (member A is subjected to axial compression and bending – beam-column), is triggered by the lateral-torsional instability of the beam (member B).

(v) The critical buckling mode shapes of the LF-U and PF-C frames exhibit practically null joint deformations (*i.e.*, displacements of the point corresponding to the intersection of the converging

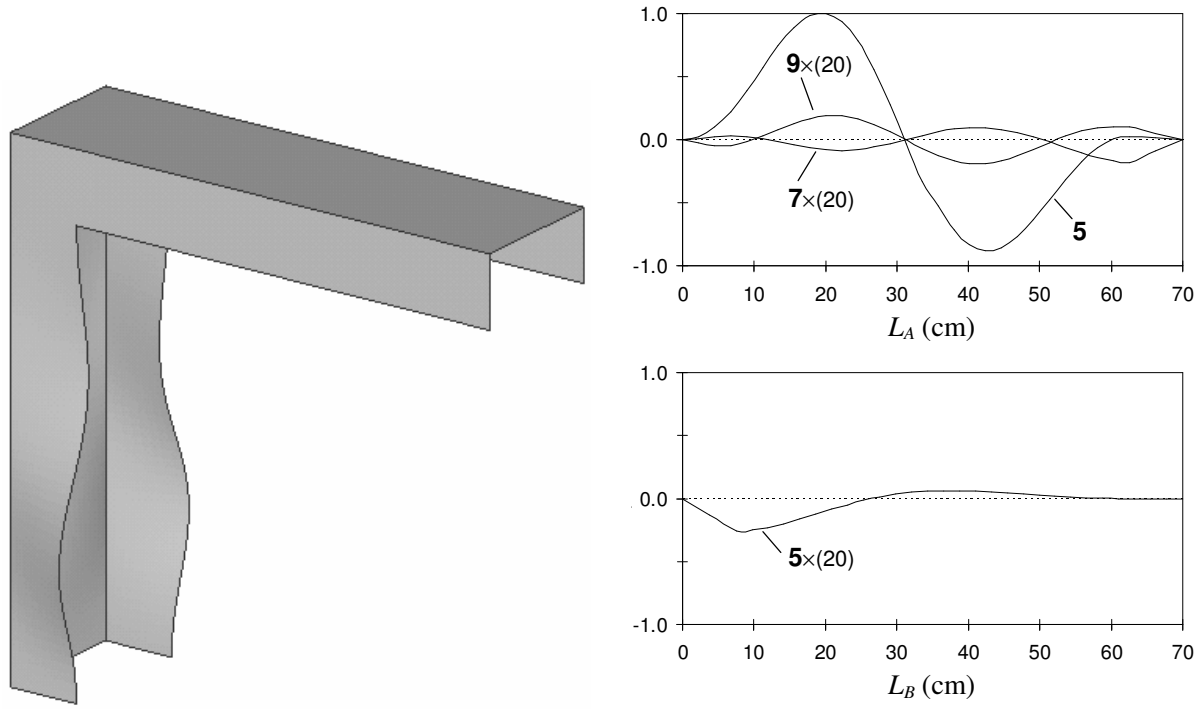


Figure 8: – LF-U frame: ANSYS and GBT critical buckling mode representations.

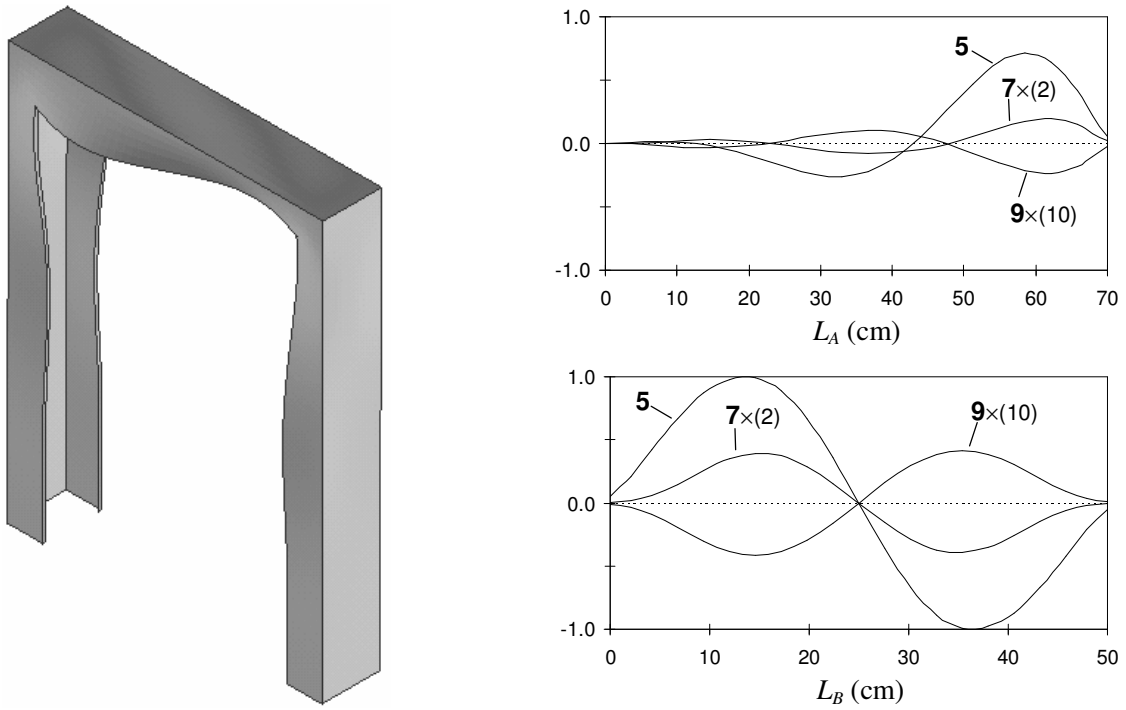


Figure 9: – SF-C frame: ANSYS and GBT critical buckling mode representations.

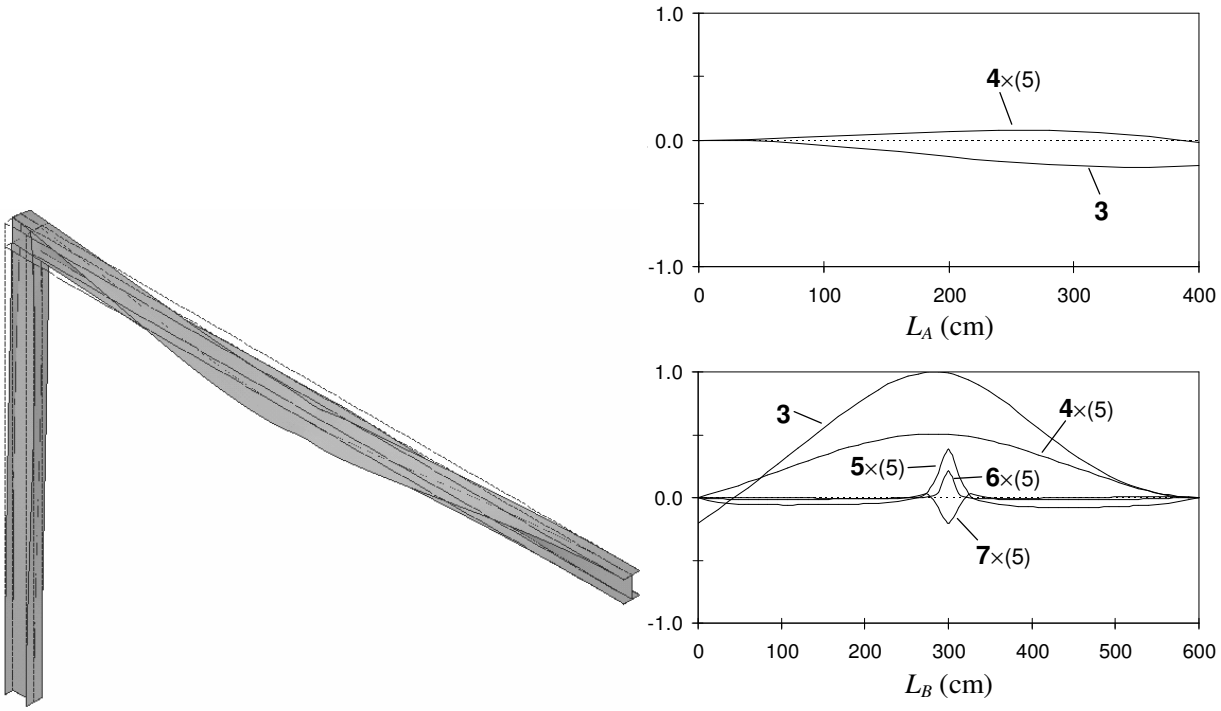


Figure 10: – LF-I frame: ANSYS and GBT critical buckling mode representations.

member centroidal axes). However, significant out-of-plane displacements, which stem from the beam lateral-torsional buckling (recall that the frame joint is not restrained against out-of-plane displacements), occur in the close vicinity of the LF-I frame joint.

In order to establish the frame critical buckling mode "dominant natures", it is necessary to perform GBT analyses that including only global, distortional or local deformation modes. Table 1 shows the ratios between the "pure" global ($Q_{b.e}$), distortional ($Q_{b.d}$) and local ($Q_{b.l}$) buckling loads and $Q_{cr.GBT}$. Then, the frame "dominant buckling mode nature", given in the last column, reflects that the corresponding "pure" buckling load is the closest to $Q_{cr.GBT}$ (*i.e.*, corresponds to the the lowest of the three ratios).

Table 1: Relation between the $Q_b$ and $Q_{cr}$ load values.

| *Frame* | $Q_{b.e}/Q_{cr}$ | $Q_{b.d}/Q_{cr}$ | $Q_{b.l}/Q_{cr}$ | *Dominant buckling mode nature* |
|---|---|---|---|---|
| LF-U | 26.75 | – | 1.00 | Local |
| PF-C | 5.22 | 1.03 | 1.52 | Distortional |
| LF-I | 1.05 | – | 1.71 | Global |

## 4. Post-Buckling Results

This section addresses the SFE analysis of the elastic and elastic-plastic (for yield stress values equal to $f_y$=*250,450,650MPa*) post-buckling behaviors of the LF-U, PF-C and LF-I frames. The curves shown in Figs. 11(a), 12(a) and 13(a) are the post-buckling equilibrium paths *Q vs.* $v_1$, *Q vs.* $v_2$ and *Q vs.* $\theta$, where (i) the symbols □, △ and ○ identify the limit equilibrium states corresponding to the ultimate loads, (ii) $v_1$ and $v_2$ are the transverse displacements of points $P_1$ (LF-U frame) and $P_2$ (PF-C frame), selected in order to provide a better frame post-buckling characterization (Figs. 11(a) and 12(a) show the location of these points), and (iii) $\theta$ is the torsional rotation of the beam mid-span cross-section (LF-I frame). As for Figs. 11(b), 12 (b) and 13(b), they provide the failure modes and von Mises stress distributions of three frames: (i) LF-U frame with $f_y$=*250MPa*, (ii) PF-C frame with $f_y$=*450MPa* and (iii) LF-I frame with $f_y$=*650MPa* – note that Fig. 12(b) also includes detailed information showing the onset of yielding. The observation of the post-buckling results shown in Figs. 11 to 13 leads to the following conclusions:

(i) Naturally, the amount of post-critical strength reserve increases ($i_1$) with the yield stress (obviously) and ($i_2$) in the frame sequence as LF-I (global buckling), PF-C (distortional buckling), LF-U (local buckling). The higher post-critical strength reserve, occurring for the LF-U frame with $f_y$=*650MPa*, corresponds to an ultimate-to-critical load ratio equal to *1.90*.

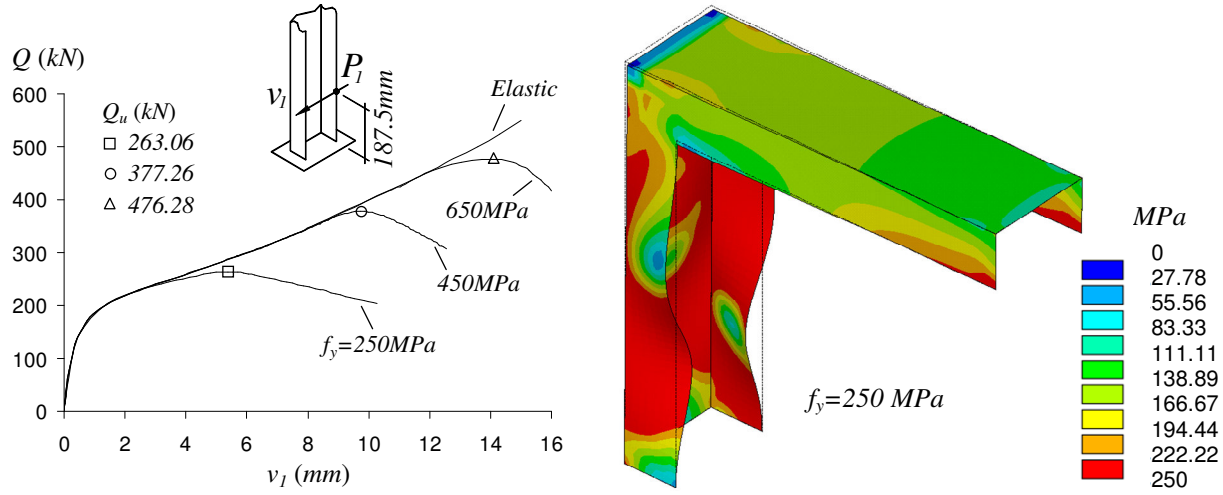


Figure 11: LF-U frame (a) post-buckling equilibrium paths and (b) deformed configuration plus von Mises stresses at collapse.

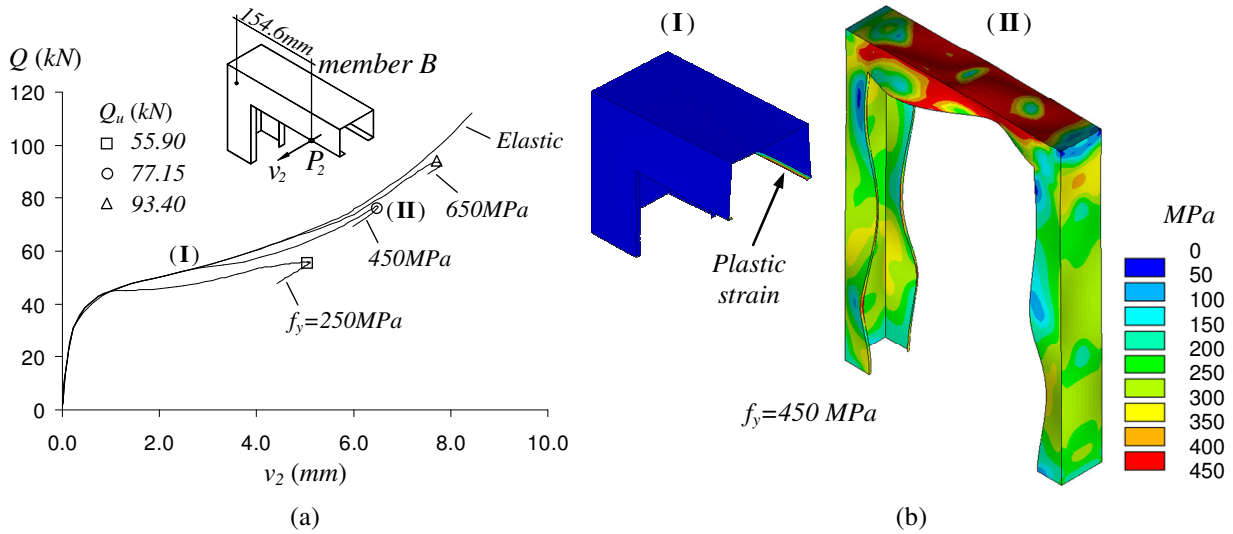


(a) (b)

Figure 12: PF-C frame (a) post-buckling equilibrium paths and (b) detail of the onset of yielding and deformed configuration plus von Mises stresses at collapse.

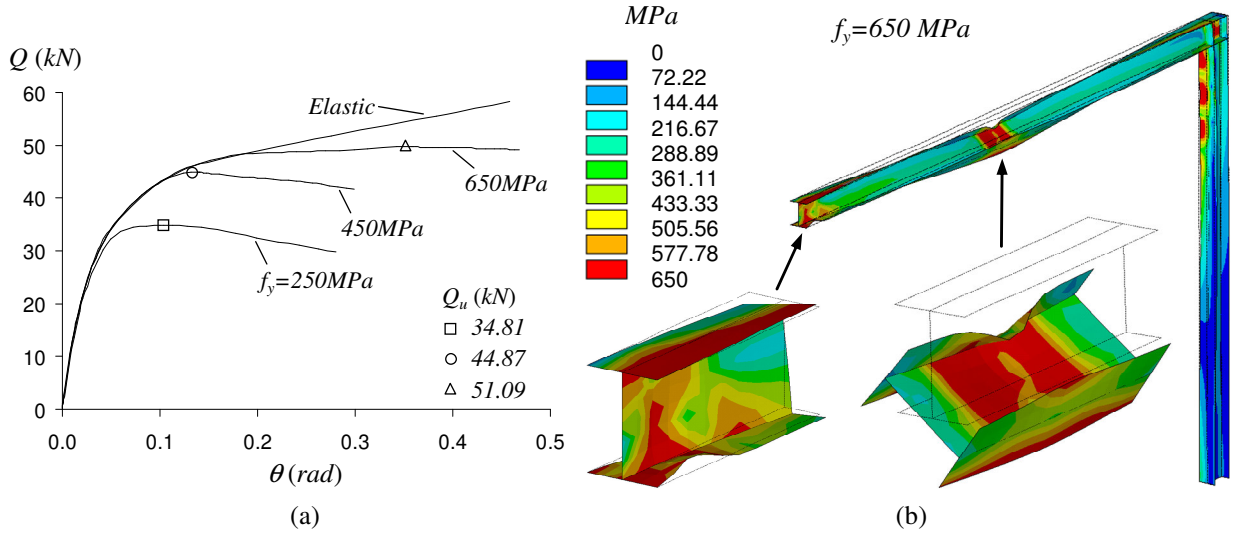


(a) (b)

Figure 13: LF-I frame (a) post-buckling equilibrium paths and (b) deformed configuration plus von Mises stresses at collapse.

(ii) Increasing the yield stress from *250MPa* to *650MPa* leads to ultimate load increases of *81%* (LF-U frames), *67%* (PF-C frames) and *47%* (LF-I frames).

(iii) The members responsible for the frame collapse are those triggering its instability, *i.e.*, member A (LF-U frames), member B (PF-C frames) and the beam (LF-I frames).

(iv) As shown in Fig. 12(b), the onset of yielding in the PF-C frame with $f_y$*=450MPa* occurs for the load *Q=52.30kN* (equilibrium state **I**) and plasticity first appears at the member lips and in the vicinity of the frame joint. The collapse occurs considerably after, for *Q=77.15kN* (equilibrium state **II**), and is precipitated by the full yielding of the member B central region.

(v) While the LF-U and PF-C frame failure mechanisms are very similar to the corresponding critical buckling mode shapes (predominantly local and distortional collapses – see Figs. 11(b) and 12(b)), the LF-I frame with $f_y$*=650MPa* (highest yield stress) fails in a mode exhibiting significant local deformations, occurring mainly in the vicinity of the beam end support and point of load application – such local deformations are practically absent from the frame critical buckling mode (see Fig. 10).

## 5. DSM Design Procedure

The current DSM adopts "Winter-type" design curves, calibrated against experimental and numerical results concerning the ultimate strengths of single-span columns and beams under uniform compression and bending (*e.g.*, Schafer 2008). The ultimate strength estimates ($P_n$ for columns and $M_n$ for beams) against local ($P_{nl}$, $M_{nl}$), distortional ($P_{nd}$, $M_{nd}$) and global ($P_{ne}$, $M_{ne}$) failures are obtained on the basis of the (i) elastic buckling loads ($P_{crl}$, $P_{crd}$ and $P_{cre}$) or moments ($M_{crl}$, $M_{crd}$ and $M_{cre}$), and (ii) either the cross-section yield load ($P_y$) and fist-yield moment ($M_y$) or the column/beam global strength ($P_{ne}$ or $M_{ne}$ – local/global interactive failure). The expressions providing $P_{ne}$, $P_{nl}$, $P_{nd}$, $M_{ne}$, $M_{nl}$ and $M_{nd}$ are given by

$$P_{ne} = \left(0.658^{\lambda_{c.e}^2}\right) P_y \quad \text{if} \quad \lambda_{c.e} = \sqrt{P_y / P_{cre}} \le 1.5$$

$$P_{ne} = \left(\frac{0.877}{\lambda_{c.e}^2}\right) P_y \quad \text{if} \quad \lambda_{c.e} > 1.5 \quad , \quad (1)$$

$$P_{nl} = P_{ne} \quad \text{if} \quad \lambda_{c.l} = \sqrt{P_{ne} / P_{crl}} \le 0.776$$

$$P_{nl} = \left(1 - 0.15\left(\frac{P_{crl}}{P_{ne}}\right)^{0.4}\right)\left(\frac{P_{crl}}{P_{ne}}\right)^{0.4} P_{ne} \quad \text{if} \quad \lambda_{c.l} > 0.776 \quad , \quad (2)$$

$$P_{nd} = P_y \quad \text{if} \quad \lambda_{c.d} = \sqrt{P_y / P_{crd}} \le 0.561$$

$$P_{nd} = \left(1 - 0.25\left(\frac{P_{crd}}{P_y}\right)^{0.6}\right)\left(\frac{P_{crd}}{P_y}\right)^{0.6} P_y \quad \text{if} \quad \lambda_{c.d} > 0.561 \quad , \quad (3)$$

$$M_{ne} = M_y \quad \text{if} \quad \lambda_{b.e} = \sqrt{M_y / M_{cre}} < 0.60$$

$$M_{ne} = \frac{10}{9}\left(1 - \frac{10 M_y}{36 M_{cre}}\right) M_y \quad \text{if} \quad 0.60 \le \lambda_{b.e} \le 1.336$$

$$M_{ne} = M_{cre} \quad \text{if} \quad \lambda_{b.e} > 1.336 \quad , \quad (4)$$

$$M_{nl} = M_{ne} \quad \text{if} \quad \lambda_{b.l} = \sqrt{M_{ne} / M_{crl}} \le 0.776$$

$$M_{nl} = \left(1 - 0.15\left(\frac{M_{crl}}{M_{ne}}\right)^{0.4}\right)\left(\frac{M_{crl}}{M_{ne}}\right)^{0.4} M_{ne} \quad \text{if} \quad \lambda_{b.l} > 0.776 \quad , \quad (5)$$

$$M_{nd} = M_y \quad \text{if} \quad \lambda_{b.d} = \sqrt{M_y / M_{crd}} \le 0.673$$

$$M_{nd} = \left(1 - 0.22\left(\frac{M_{crd}}{M_y}\right)^{0.5}\right)\left(\frac{M_{crd}}{M_y}\right)^{0.5} M_y \quad \text{if} \quad \lambda_{b.d} > 0.673 \quad , \quad (6)$$

where (i) $\lambda_l$, $\lambda_d$ and $\lambda_e$ are the *local*, *distortional* and *global* slenderness values, (ii) $P_y=A_g.f_y$ and (iii) $M_y=W_y.f_y - A_g$ and $W_y$ are the cross-section area and elastic modulus.

In frames, like in other structural systems or in single-span members not subjected to uniform compression or bending, the various "$P_{cr}$ and $M_{cr}$ values" appearing in (1)-(6) (i) cannot adequately describe the loading and (ii) need to be replaced by "critical buckling load parameter values $Q_{cr}$". Moreover, it is worth noting that the above DSM strength curves neglect both the (i) cross-section elastic-plastic strength reserve and (ii) bending moment redistribution. Therefore, a more rational approach, already proposed by the authors in the context of continuous beams (Basaglia and Camotim 2012), consists of replacing the first-yield (cross-section elastic strength) load ($P_y$) or moment ($M_y$) by the "load parameter value associated with the frame (geometrically linear) plastic collapse" ($Q_{pl}$) in (1)-(6) – note that, in the case of statically determinate frames, $Q_{pl}$ corresponds to the cross-section plastic strength.

In order to be able to assess the quality of the frame ultimate strength estimates provided by the proposed DSM approach, described in the previous paragraph, the first step consists of determining the $Q_{pl}$ values for the LF-U, PF-C and LF-I frames, all assumed to exhibit *6* different yield stresses, namely $f_y=250,300,350,450,550,650MPa$. These $Q_{pl}$ values were obtained through first-order elastic-plastic

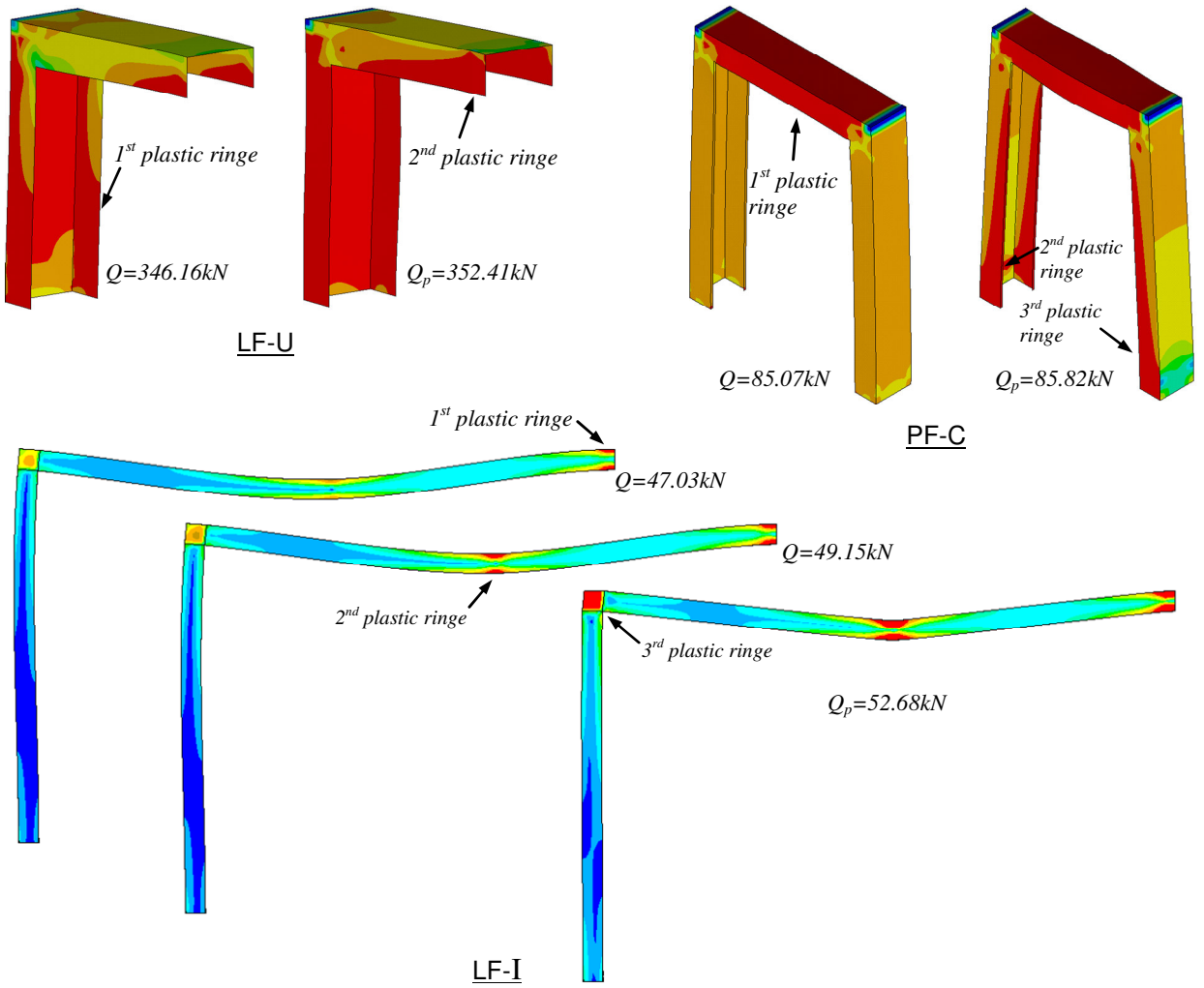


Figure 14: First-order elastic-plastic deformed configurations and von Misses stress distribution concerning the LF-U, SF-C and LF-I frames with $f_y=250MPa$ and corresponding to their (i) plastic hinge formations and (ii) collapses.

ANSYS SFEA and are given in Table 2. For illustrative purposes, Fig. 14 displays deformed configurations and von Mises stress distributions, concerning the three frames analyzed and $f_y$=250MPa, which are associated with (i) the formation of the successive "plastic hinges" (cross-section full yielding) and (ii) the frame collapse. Note that the members triggering the frame instabilities are again those also responsible for their (first-order) plastic collapses. Moreover, since the LF-U and PF-C frame members are almost exclusively subjected to axial compression, the corresponding first plastic hinge locations are not well defined at all – indeed, full yielding occurs practically at the same time in a whole member "region". Conversely, the first plastic hinge location is very well defined in the LF-I frame, as it occurs at the beam end support – in this case, beam non-uniform bending is the primary action (for instability and collapse).

Next, the ultimate load estimates yielded by the DSM approach are compared with the ANSYS SFE values, for the three frames with yield stresses $f_y$=250,300,350,450,550,650MPa. As mentioned earlier, the current DSM prescribes different strength curve sets for columns (Eqs. (1)-(3)) and beams (Eqs. (4)-(6)). In this work, the DSM curve set selection was made on the basis of the member triggering the frame instability and collapse (the same in all cases). This means that DSM column strength curves to be considered concern (i) columns for the LF-U and PF-C frames, and (ii) beams for the LF-I frames[2].

Table 2: Comparison between the beam ultimate load "exact" values and DSM estimates.

| | | | SFEA | | | DSM | | | | |
|---|---|---|---|---|---|---|---|---|---|---|
| | $f_y$ ($MPa$) | DBN | $Q_{pl}$ ($kN$) | $Q_u$ ($kN$) | $\lambda_{cr.pl}$ | $Q_{u.DSM}$ ($kN$) | $Q^*_{u.DSM}$ ($kN$) | FMN | $\frac{Q_{u.DSM}}{Q_u}$ | $\frac{Q^*_{u.DSM}}{Q_u}$ |
| LF-U | 250 | L | 352.41 | 263.06 | 1.18 | 264.95 | 264.95 | L/G | 1.01 | 1.01 |
| | 300 | L | 423.12 | 293.79 | 1.29 | 298.01 | 298.01 | L/G | 1.01 | 1.01 |
| | 350 | L | 493.03 | 322.72 | 1.39 | 328.47 | 328.47 | L/G | 1.02 | 1.02 |
| | 450 | L | 634.64 | 377.27 | 1.58 | 384.86 | 384.86 | L/G | 1.02 | 1.02 |
| | 550 | L | 774.28 | 428.19 | 1.74 | 435.16 | 435.16 | L/G | 1.02 | 1.02 |
| | 650 | L | 916.78 | 476.28 | 1.90 | 482.29 | 482.29 | L/G | 1.01 | 1.01 |
| PF-C | 250 | D | 85.82 | 55.90 | 1.29 | 51.62 | 51.62 | D | 0.92 | 0.92 |
| | 300 | D | 103.67 | 61.69 | 1.42 | 57.02 | 57.02 | D | 0.92 | 0.92 |
| | 350 | D | 121.07 | 66.81 | 1.53 | 61.74 | 61.74 | D | 0.92 | 0.92 |
| | 450 | D | 155.89 | 77.15 | 1.74 | 70.00 | 70.00 | D | 0.91 | 0.91 |
| | 550 | D | 190.27 | 85.82 | 1.92 | 77.07 | 77.07 | D | 0.90 | 0.90 |
| | 650 | D | 224.64 | 93.40 | 2.09 | 83.38 | 83.38 | D | 0.89 | 0.89 |
| LF-I | 250 | G | 52.68 | 34.81 | 1.01 | 41.84 | 41.84 | G | 1.20 | 1.20 |
| | 300 | G | 63.54 | 38.79 | 1.11 | 46.32 | 46.32 | G | 1.19 | 1.19 |
| | 350 | G | 73.36 | 41.10 | 1.20 | 49.14 | 49.14 | G | 1.20 | 1.20 |
| | 450 | G | 93.39 | 44.87 | 1.35 | 51.32 | 50.90 | L/G | 1.14 | 1.13 |
| | 550 | G | 115.89 | 46.99 | 1.50 | 51.32 | 50.90 | L/G | 1.09 | 1.08 |
| | 650 | G | 137.10 | 51.10 | 1.63 | 51.32 | 50.90 | L/G | 1.01 | 1.00 |

[2] Note that, since the current DSM does not cover beam-columns, the DSM strength curve selection procedure employed in this work would be "irreparably compromised" if the instability and collapse of the LF-I frames was triggered by member A, which is a beam-column – at least, until DSM beam-column strength curves are developed and adequately validated.

Since some of the frames may exhibit "mixed" buckling and failure modes, the DSM estimates obtained were based on two concepts: (i) failure mode nature assumed to coincide with the "dominant buckling mode nature" (see Table 1) and slenderness values based on the frame "real" critical buckling load $Q_{cr}$, corresponding to a "mixed" buckling mode (not local, distortional or global), and (ii) lower of $Q_{ne}$, $Q_{nl}$, $Q_{nd}$ and the three slenderness values based on $Q_{cr.i}=(Q_{b.i}/Q_{b.min})\times Q_{cr}$, where $Q_{b.min}=\min\{Q_{b.e},Q_{b.d},Q_{b.l}\}$ – usual DSM application. Table 2 provides, for all the frames analyzed, the following values: (i) first-order plastic collapse ($Q_{pl}$) and ultimate ($Q_u$) loads, (ii) critical slenderness values ($\lambda_{cr.pl}$), obtained from $Q_{cr}$ (given in section 3) and $Q_{pl}$, (iii) ultimate load estimates yielded by the current DSM design curves ($iii_1$) selected on the basis of the dominant buckling nature ($Q_{u.DSM}$) and ($iii_2$) corresponding to the lower of $Q_{ne}$, $Q_{nl}$, $Q_{nd}$ ($Q^{*}_{u.DSM}$). Moreover, this table provides also (i) the dominant buckling natures (DBN),

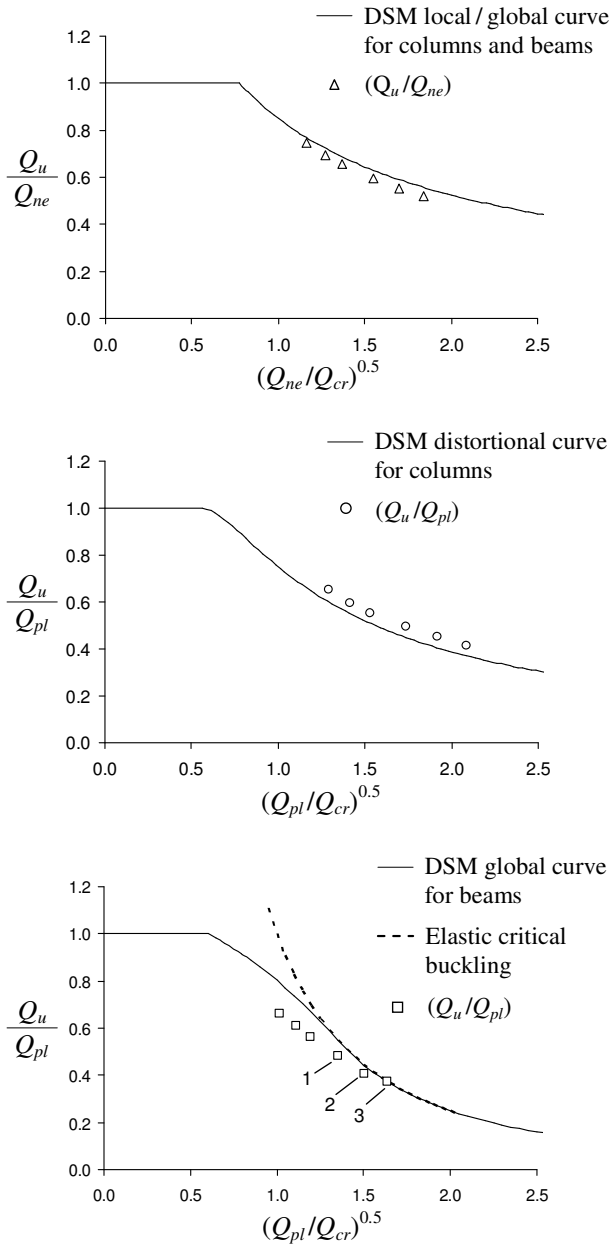


Figure 15: DSM ultimate load estimates and SFE values: "dominant buckling mode nature"

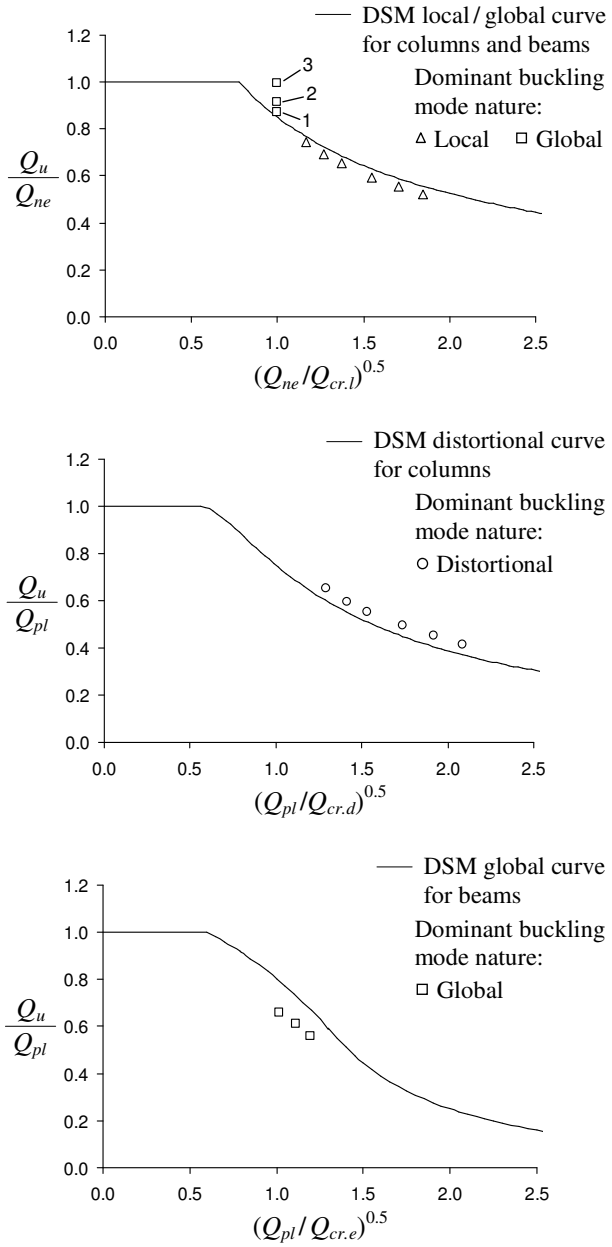


Figure 16: DSM ultimate load estimates and "SFE values: minimum of $Q_{ne}$, $Q_{nl}$, $Q_{nd}$

(ii) the failure mode natures predicted by the DSM (FMN) and (iii) the values of the ratios $Q_{u.DSM}/Q_u$. On the other hand, Figs. 15 and 16 make it possible to compare the above two sets of DSM estimates with the values obtained by means of the ANSYS SFE analyses – the small triangles, circles and squares identify the LF-U, PF-C and LF-I frame numerical ultimate strengths, respectively.

The observation of the results presented in Table 2 and Figs. 15-16 prompts the following comments and remarks, concerning the "quality" of the DSM-based frame ultimate strength estimates:

(i) The comparison between the SFE ultimate load values and the corresponding DSM estimates based on the "dominant buckling mode nature", both of which are displayed in Fig. 15, makes it possible to conclude that ($i_1$) the LF-U frame predictions (local instability/collapse) are all very accurate, even if minutely unsafe ($Q_{u.DSM}/Q_u$ values varying between *1.01* and *1.02*), ($i_2$) the PF-C frame predictions (distortional instability/collapse) are all safe, even if only reasonable accurate ($Q_{u.DSM}/Q_u$ values varying between *0.89* and *0.92*), and ($i_3$) the LF-I frame predictions (global instability/collapse) are practically all fairly or excessively unsafe (with a single exception, which corresponds to a "perfect" estimate, the $Q_{u.DSM}/Q_u$ values vary between *1.09* and *1.20*).

(ii) The adoption of the lower of the $Q_{ne}$, $Q_{nl}$, $Q_{nd}$ values as the frame ultimate strength estimate only leads to a change in three LF-I frames, namely those associated with higher slenderness values, *i.e.*, yield stresses. They correspond to the points labeled **1**-**3** in the bottom plot of Fig. 15, which are found to "migrate" to the bottom plot of Fig. 16, thus meaning that the current DSM application predicts local/global interactive failures for these three frames. Note also that their slenderness values, which change from global to local, ($ii_1$) are substantially reduced and ($ii_2$) become identical, which stems from the fact that $Q_{ne}=Q_{cre}$ for $\lambda_{b.e}>1.336$ and, thus, $\lambda_{b.l}=(Q_{cre}/Q_{crl})^{0.5}$ is constant (see (4)-(5)).

(iii) Since $Q_{crl}$ is considerably larger than $Q_{cre}$ for the three frames identified in the previous item, the local/global interaction effects are rather weak, which explains the extreme closeness between the $Q^*_{u.DSM}$ and $Q_{u.DSM}$ values, leading to (minuscule) differences in the corresponding ultimate strength ratios (see the last three rows in Table 2) – the $Q^*_{u.DSM}$ values are a touch below the $Q_{u.DSM}$ ones. So, in this particular case, the DSM global and local/global interactive strength curves predict essentially the same failure loads, but on the basis of distinct slenderness values.

(iv) The natures of the collapse modes displayed in Figs. 11 (LF-U frame with $f_y=250MPa$), 12 (PF-C frame with $f_y=450MPa$) and 13 (LF-I frame with $f_y=650MPa$) confirm the DSM predictions. Indeed, while the first two frames exhibit pure local and distortional collapse modes, respectively, the third one fails in a mode that combines local and global (flexural-torsional) deformations.

(v) The ultimate strengths of two LF-I frames predicted to fail in local/global interactive modes (those with critical slenderness values higher than *1.5*) are fairly well estimated by the elastic critical buckling curve[3], thus confirming the findings recently reported by the authors (Basaglia & Camotim 2012) in the context of two and three-span continuous beams. Indeed, the elastic critical buckling curve overestimates these two ultimate strengths by *9%* ($\lambda_{cr.pl}=1.5$) and *1%* ($\lambda_{cr.pl}=1.63$), respectively.

(vi) Due to time limitations, only frames with moderate-to-high critical slenderness values were analyzed. Results for frames with low, low-to-moderate and high slenderness values will be reported soon.

## 6. Concluding Remarks

This work reported the results of an ongoing numerical investigation on the local, distortional and global buckling, post-buckling, collapse and DSM design of simple frames. These results consisted of (i) critical

[3] Recall that the current DSM beam global strength curve coincides with the elastic critical buckling curve for $\lambda_{b.e}>1.336$.

buckling loads and mode shapes, determined through GBT and ANSYS analyses, (ii) post-buckling equilibrium paths (up to collapse), deformed configurations and von Mises stress distributions, obtained by means of ANSYS elastic and elastic-plastic SFE analyses, and (iii) ultimate load estimates, provided by the current DSM strength curves. Out of the findings unveiled in the course of this work, the following ones deserve to be specially mentioned:

(i) The frame buckling modes often exhibit a "mixed" nature, thus precluding its direct classification as local, distortional or global. Therefore, it is necessary to resort to the "dominant buckling mode nature" concept in order to classify the buckling modes– the use of GBT-based buckling analyses makes the application of this concept fairly straightforward.

(ii) Since the (modified) current DSM strength curves were developed and validated in the context of isolated columns or beams, it was expected that they would only provide satisfactory (safe and reasonably accurate) ultimate strength estimates in frames that buckle and fail in modes triggered by members subjected exclusively to pre-buckling axial compression (columns) or bending (beams) – *i.e.*, not beam-columns (members subjected to pre-buckling axial compression and bending).

(iii) Confirming the above assertion, the DSM column design curves predicted fairly well the ultimate strengths of the LF-U and PF-C frames, which ($iii_1$) buckle in "practically pure" local and distortional modes, respectively, and ($iii_2$) can be more adequately described as "rigidly connected column sets" – all its members were subjected exclusively to axial compression. All the local and distortional failure loads were slightly overestimated and underestimated, respectively.

(iv) In the LF-I frames, which ($iv_1$) included one beam and one beam-column, and ($iii_2$) buckled and failed in predominantly global modes triggered by the beam, the DSM beam strength curves overestimated the numerical failure loads by an amount that decreased with the frame global slenderness. For three frames, the lower DSM predictions corresponded to local/global interactive failures (even if the ultimate strengths obtained were only marginally lower than their global counterparts), which matched the collapse modes obtained by means of the shell finite element analyses.

Finally, it is worth noting that the work reported in this paper is just "the first step of a long journey", since a vast amount if research is obviously needed before a direct strength approach for the design of thin-walled frames can be established on solid grounds. In particular, it is necessary to come up with a fresh methodology to handle frames whose buckling and failure are triggered by members subjected to compression and bending, a task directly linked to the development of DSM-based strength curves and/or methodologies for the design isolated thin-walled beam-columns.

## Acknowledgments

The authors gratefully acknowledge the financial support of "*Fundação para a Ciência e Tecnologia*" (FCT – Portugal), through the research project "Generalised Beam Theory (GBT) – Development, Application and Dissemination" (PTDC/ECM/108146/2008) project. Moreover, the first author is also indebted to FCT for having granted him the post-doctoral scholarship nº SFRH/BPD/62904/2009.

## References

American Iron and Steel Institute (AISI) (2007). *North American Specification for the Design of Cold-Formed Steel Structural Members* (NAS: AISI-S100-07), Washington (DC).

Basaglia C, Camotim D, Silvestre N (2010). "GBT-Based Buckling Analysis of Thin-Walled Steel Frames with Arbitrary Loading and Support Conditions", *International Journal of Structural Stability and Dynamics*, **10**(3), 363-385.

Basaglia C, Camotim D (2012). "Buckling, post-buckling, strength and DSM design of cold-formed steel continuous lipped channel beams", *Journal of Structural Engineering* (ASCE), accepted for publication.

Basaglia C, Camotim D, Silvestre N (2012). "Torsion warping transmission at thin-walled frame joints: kinematics, modelling and structural response", *Journal of Construction Steel Research*, **69**, 39-53.

Bijlaard F, Feldmann M, Naumes J, Sedlacek G (2010). "The "general method" for assessing the out-of-plane stability of structural members and frames and the comparison with alternative rules in EN 1993 – Eurocode 3 – Part 1-1", *Steel Construction – Design and Research*, **3**(1), 19-33.

Camotim D, Silvestre N, Basaglia C, Bebiano R (2008). "GBT-based buckling analysis of thin-walled members with non-standard support conditions", *Thin-Walled Structures*, **46**(7-9), 800-815.

Camotim D, Basaglia C, Silvestre N (2010). "GBT buckling analysis of thin-walled steel frames: a state-of-the-art report", *Thin-Walled Structures*, **48**(10-11), 726-743.

Comité Européen de Normalisation (CEN) (2005). *Eurocode 3 – Design of Steel Structures – Part 1-1: General Rules and Rules for Buildings*, EN1993-1-1, Brussels.

Dubina D (2008). "Structural analysis and design assisted by testing of cold-formed steel structures", *Thin-Walled Structures*, **46**(7-9), 741-764.

Hancock GJ, Kwon YB, Bernard ES (1994). "Strength design curves for thin-walled sections undergoing distortional buckling." *Journal of Constructional Steel Research*, **31**(2-3), 169-186.

SAS (Swanson Analysis Systems Inc.) (2009). *ANSYS Reference Manual* (version 12).

Schafer BW, Peköz T (1998). "Direct strength prediction of cold-formed steel members using numerical elastic buckling solutions", *Proceedings of 14th International Specialty Conference on Cold-Formed Steel Structures* (St. Louis, 15-16/10), R. LaBoube, W.W. Yu (eds.), 69-76.

Schafer BW (2008). "Review: the direct strength method of cold-formed steel member design", *Journal of Constructional Steel Research*, **64**(7-8), 766-778.

Standards of Australia (2005). *Cold-Formed Steel Structures*, Australian Standard/New Zealand Standard 4600 (AS/NZS4600), Sydney.